# Dielectric and Geometric Dependence of Electric Field and Power Distribution in a Waveguide Heterogeneously Filled with Lossy Dielectrics

Lhoussain Outifa, Michel Delmotte, and Henri Jullien

***Abstract*— In microwave processing of dielectric materials which completely fill a waveguide, the distribution of the electric field within the material needs to be known. This paper presents the theoretical conditions for the microwave cure of large pieces, the size of which is more than the wavelength. The mathematical description of heterogeneously multilayer-filled waveguides presents certain difficulties because of the involved transcendental equations. A computer treatment to determine the electric-field spatial distribution is developed. The influence of the dielectric constants and the thickness of the dielectric materials on the spatial distribution of the electric field and power flow in each layer is studied. In particular, the field strength is enhanced in the dielectric with the highest permittivity. A numerical resolution of the transcendental equations defining the cutoff frequencies of propagation modes allows one to enumerate the modes, which can successively appear in a dielectric-loaded waveguide as functions of dielectric and geometric parameters. The attenuation constant and the microwave power dissipated in each material are determined. A balance sheet of energy is established.**

## I. Nomenclature

- $\alpha$ Attenuation constant.
- $\beta$ Phase constant ( $\beta = \frac{2\pi}{\lambda_g}$).
- $\gamma$ Propagation constant ($\gamma = \alpha + j\beta$).
- $\varepsilon_0$ Permittivity in vacuum.
- $\varepsilon$ Relative complex dielectric permittivity ($\varepsilon = \varepsilon' - j\varepsilon''$).
- $\varepsilon'$ Relative dielectric permittivity.
- $\varepsilon''$ Relative absorption factor (or loss factor).
- $\lambda_0$ Free space wavelength.
- $\lambda_c$ Cutoff wavelength.
- $\lambda_g$ Wavelength in waveguide.
- $\mu_0$ Magnetic permeability in vacuum.
- $a$ Length of the wider side of the waveguide cross section.
- $b$ Length of the shorter side of the waveguide cross section.
- $c$ Central part thickness in the dielectric filling of waveguide.
- $d$ $d = \frac{a-c}{2}$.
- $f_0$ Microwave frequency (generally 2.45 GHz).
- $f_c$ Cutoff frequency.
- $k_0$ Wave propagation constant; $k_0 = \sqrt{\omega^2 \varepsilon_0 \mu_0}$ or $\frac{2\pi}{\lambda_0}$.
- $P_0$ Input microwave power.
- $p$ Transverse propagation constant in I and III (see text).
- $q$ Transverse propagation constant in II (see text).
- $r$ $\frac{(c/a)}{1-(c/a)}$.
- $Z$ Wave impedance; $Z = \sqrt{\frac{\mu_0}{\varepsilon_0}} \frac{\lambda_g}{\lambda_0}$.

Manuscript received September 15, 1995; revised April 25, 1997. This work was supported by the Centre National de la Recherche Scientifique (CNRS/PIRSEM-ECOTECH), the Agence Française de l'Environnement et la Maîtrise de l'Energie (ADEME), Peugeot SA, Renault SA, and Electricité de France (EDF).

The authors are with the Laboratoire Microstructure et Mécanique des Matériaux, C.N.R.S. URA 1219, ENSAM F 75013 Paris, France.

Publisher Item Identifier S 0018-9480(97)05369-6.

## II. Introduction

THE USE of microwave energy for the processing of curing organic or inorganic composite materials requires a good efficiency of the electric system and a total uniformity of the spatial distribution of temperature [1]–[5]. To realize conditions of both efficiency and homogeneity, the control of heat source spatial distribution must be established. This control first requires the control of electric-field distribution [6]–[9]. This paper describes the basic data of this control in a dielectric-loaded traveling-wave applicator, in which the dominant mode $\mathrm{TE}_{01}$ is realized. This mode allows the largest volumes with a homogeneous field distribution of the electric field [6], [7] to be obtained.

Theoretical treatments of dielectric-loaded waveguides can be found [10]–[15] because of the technologic interest of their impedance characteristics in complex propagation systems (phase shifters, for instance), but are restricted to nondissipating materials (absorption factor is equal to zero) and concern telecommunication applications (waveguide devices). This paper is outside of this area, but it appears that the question of energy transfer to dielectric lossy materials by means of microwave systems requires the study of the electromagnetic (EM) propagation in specific applicators used for material processing.

In convenient applications of the microwave power, the load materials, and especially the material to be transformed, are dissipating so that the microwave power is converted into heat. In such a case, electric-field and microwave-power spatial distributions are not well known and, as it might be expected, present certain difficulties which do not arise with lossless materials. Consequently, there is an urgent need to establish a theoretical background for this type of microwave power use.

The dielectric characteristics ($\varepsilon'$, $\varepsilon''$) of the material to cure are the main basis; the objectives of the theoretical developments are to select load dielectrics (for instance, in the microwave processing of composite materials, the material to

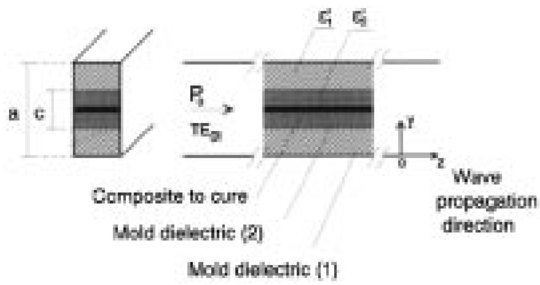


Fig. 1. Cross-sectional and longitudinal view of the applicator loaded with the curing composite inserted inside a mold made of two dielectrics.

be performed is sandwiched between a number of dielectric layers above and below) in order to obtain both a satisfactory homogeneity of the transformation and the energy optimization of the process. It must be noticed that the dielectric absorption factors of mold materials used in the process are weak; the material to cure is the dielectric with the highest absorption factor.

In this paper, the electric-field and microwave-power spatial distributions are studied versus the size and the permittivities of materials. The conditions for only the dominant mode to be selected are determined. The attenuation constant and the density of absorbed power in a waveguide inhomogeneously filled with lossy dielectrics are established.

## III. Theoretical Analysis of the Structure

The experimental microwave applicator studied in this work consists of a rectangular guide, standard or nonstandard, oversized or not, related to the size of the objects to cure. The guide is loaded with a number of dielectric layers as shown in Fig. 1, such as the interfaces between dielectric layers are parallel to the electric-field vector $\mathbf{E}$. The material to be transformed is placed in the middle of the applicator, where the electric field is maximum, and inside a dielectric layer the permittivity $\varepsilon_2'$ of which is the same as the permittivity of the material to be transformed. This dielectric layer is typically *the mold*. Above and below this median part, dielectric layers are characterized by their permittivity $\varepsilon_1'$, with $\varepsilon_1'/\varepsilon_2' < 1$ according to the electric-field focusing considerations developed below. It follows that in a first step the simplified Fig. 2 can be considered.

### A. Electric-Field Distribution

In this section, the electromagnetic (EM) wave propagation in the structures shown in Figs. 1 and 2 will be analyzed, starting with the following Maxwell's equations:

$$\nabla \times \mathbf{E} = -\mu \frac{\partial \mathbf{H}}{\partial \mathbf{t}}$$
$$\nabla \times \mathbf{H} = \varepsilon \frac{\partial \mathbf{E}}{\partial t}.$$

In general, the propagation modes in this structure are neither TE nor TM, but a combination of both, hence their name of hybrid modes [10]–[12]. However, considerations of the boundary conditions lead to the fact that when there is no variation of the electric-field component in the $Ox$-direction,

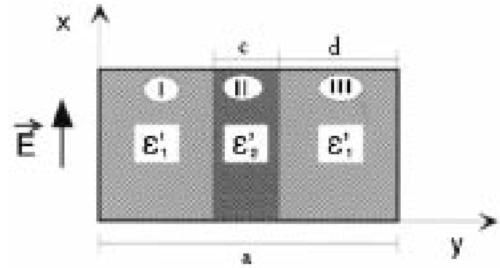


Fig. 2. Cross section of the applicator loaded with two dielectrics.

only TE modes are to be considered [13]–[15], [19]. Thus, for $\mathrm{TE}_{0n}$ modes, the development of Maxwell's equations in the three dielectric layers of Fig. 2 leads to the following differential equations that $\mathbf{E_x}$ satisfies:

in regions I and III:

$$\frac{d^2\mathbf{E_x(y)}}{dy^2} + (\varepsilon_1' k_0^2 - \beta^2)\mathbf{E_x(y)} = \mathbf{0} \qquad (1)$$

in region II:

$$\frac{d^2\mathbf{E_x(y)}}{dy^2} + (\varepsilon_2' k_0^2 - \beta^2)\mathbf{E_x(y)} = \mathbf{0} \qquad (2)$$

with $k_0^2 = \omega^2\mu_0\varepsilon_0 = (2\pi/\lambda_0)^2$ and $\beta = 2\pi/\lambda_g$, and according to the fact that the global expression of the electric field is

$$\mathbf{E_x(y,z,t)} = \mathbf{E_0}.\mathbf{E_x(y)}\mathbf{e}^{-\alpha \mathbf{z}}\mathbf{e}^{\mathbf{j}(\omega \mathbf{t} - \beta \mathbf{z})}.$$

Assuming that $\varepsilon_1'/\varepsilon_2' < 1$, the electric field is always a sinusoidal function of $y$ in II, while it can be either a sinusoidal, linear, or exponential function of $y$ in I and III depending on the sign of the quantity $\varepsilon_1' k_0^2 - \beta^2$. The three cases are detailed as follows:

$$\lambda_g > \frac{\lambda_0}{\sqrt{\varepsilon_1'}} \quad \text{sinusoidal function}$$
$$\lambda_g = \frac{\lambda_0}{\sqrt{\varepsilon_1'}} \quad \text{linear function}$$
$$\lambda_g < \frac{\lambda_0}{\sqrt{\varepsilon_1'}} \quad \text{exponential function.}$$

$\varepsilon_1' k_0^2 - \beta^2$ and $\varepsilon_2' k_0^2 - \beta^2$ are the squared normalized transverse propagation constants $p/d$ in I and III and $2q/c$ in II, respectively, where

$$(p/d)^2 = \varepsilon_1' k_0^2 - \beta^2 \qquad (3)$$
$$(2q/c)^2 = \varepsilon_2' k_0^2 - \beta^2. \qquad (4)$$

The boundary conditions are that $\mathbf{E}_{\tan}$ (i.e., $\mathbf{E_x}$) and $\mathbf{H}_{\tan}$ (i.e., $\mathbf{H_z}$) are continuous functions at the interfaces defined as $y = (a-c)/2$ and $y = (a+c)/2$. It follows that

$$(\tan p + \frac{pr}{q}\tan q)(\tan p \tan q - \frac{pr}{q}) = 0.$$

The $\mathrm{TE}_{0,n}$ modes are separated into $\mathrm{TE}_{0,\mathrm{even}}$ and $\mathrm{TE}_{0,\mathrm{odd}}$ modes. Hence, one gets

$$\frac{\tan p}{p} = -r\frac{\tan q}{q}, \qquad \text{for } \mathrm{TE}_{0,n} \text{ modes } (n \text{ even}) \qquad (5)$$
$$\frac{\tan p}{p} = r\frac{\cot q}{q}, \qquad \text{for } \mathrm{TE}_{0,n} \text{ modes } (n \text{ odd}). \qquad (6)$$

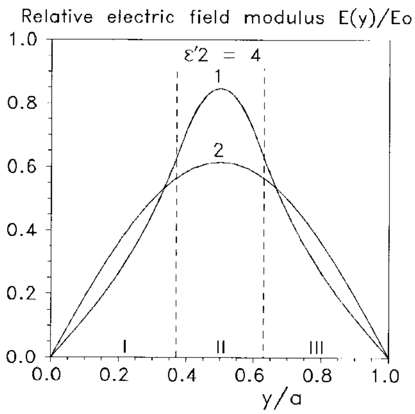


Fig. 3. Electric-field modulus profile along the larger side of the applicator, as a function of the permittivity in the dielectrics I and III ($\varepsilon_2' = 4$ in the dielectric II; $c/a = 0.27$). 1: $\varepsilon_1' = 1.1$; 2: $\varepsilon_1' = 4$.

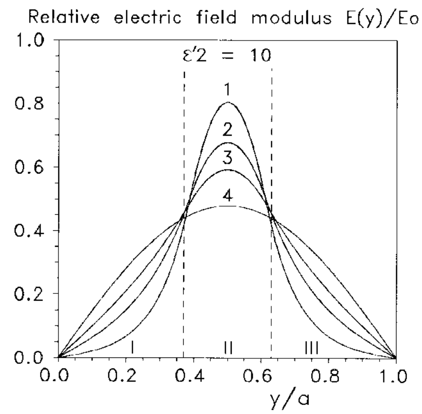


Fig. 4. Electric-field modulus profile along the larger side of the applicator, as a function of the permittivity $\varepsilon_1'$ in the dielectrics I and III ($\varepsilon_1' = 10$ in the dielectric II; $c/a = 0.27$). 1: $\varepsilon_1' = 1$; 2: $\varepsilon_1' = 6$; 3: $\varepsilon_1' = 8$; 4: $\varepsilon_1' = 10$.

Using (6) for the dominant mode $\mathrm{TE}_{01}$, and with (3) and (4), one obtains

$$\frac{\tan\left(\pi(a-c)\sqrt{\frac{\varepsilon_1'}{\lambda_0^2}-\frac{1}{\lambda_g^2}}\right)}{\sqrt{\frac{\varepsilon_1'}{\lambda_0^2}-\frac{1}{\lambda_g^2}}} = \frac{\cot\left(\pi c\sqrt{\frac{\varepsilon_2'}{\lambda_0^2}-\frac{1}{\lambda_0^2}}\right)}{\sqrt{\frac{\varepsilon_1'}{\lambda_0^2}-\frac{1}{\lambda_g^2}}}. \quad (7)$$

Solved by means of a computer treatment, this transcendental equation gives the propagation wavelength $\lambda_g$, so that the normalized eigenvalues $p$ and $q$, which are the key to all the previous field expressions, are determined.

Finally, the electric-field distribution inside the completely and heterogeneously filled waveguide is given by the following expressions:

$$\text{region I: } \mathbf{E_x(y)} = \mathbf{E_0}\sinh\left(\frac{|p|}{d}y\right)$$

$$\text{region II: } \mathbf{E_x(y)} = j\mathbf{E_0}\left(\sinh|\mathbf{p}|\cos\left(\frac{\mathbf{2}q}{c}y-\frac{q}{r}\right) + \frac{|p|r}{q}\cosh|p|\sin\left(\frac{2q}{c}y-\frac{q}{r}\right)\right)$$

$$\text{region III: } \mathbf{E_x(y)} = \mathbf{E_0}\sinh\left(\frac{|p|}{d}(a-y)\right).$$

Of course, these expressions satisfy the boundary conditions of continuity, because $p$ and $q$ are calculated values satisfying these conditions.

Typical representations of these functions are given in Fig. 3 with $\varepsilon_2' = 4$ in the central part II, and in Fig. 4 with $\varepsilon_2' = 10$. For low values of the permittivity $\varepsilon_1'$ in the peripheral dielectric, the energy is largely concentrated in the middle of the applicator, where the material to cure is located.

### *B. Microwave Power Flow in the Structure*

Since the structure is symmetrical with respect to the plan $y = a/2$, the power-flow expression can be reduced to

$$P_0 = \frac{b}{Z}\left(\int_0^d |\mathbf{E_{x;I}}|^2\,dy + \int_d^{a/2} |\mathbf{E_{x;II}}|^2\,dy\right).$$

TABLE I
VARIATION OF THE RELATIVE POWER FLOW IN THE MATERIAL TO CURE, AS A FUNCTION OF THE PERMITTIVITY $\varepsilon_1'$ IN THE OUTER PART ($\varepsilon_2' = 4$; $c/a = 0.27$)

| $\varepsilon'_1$ | 1 | 2 | 3 | 4 |
|---|---|---|---|---|
| $\frac{P_2}{P_1 + P_2}$ | 0.65 | 0.59 | 0.52 | 0.44 |

Substituting the values of $|\mathbf{E_{x;I}}|$ and $|\mathbf{E_{x;II}}|$ from the above equations for the different regions, and evaluating the integral, the total power flow becomes

$$P_0 = \frac{S|\mathbf{E_0}|^2}{4Z(1+r)}(p_1+p_2)$$

with

$$p_1 = \frac{sh2|p|}{2|p|} - 1$$

$$p_2 = r\left[\left(\frac{|p|r}{q}\right)^2(\cosh|p|)^2\left(1-\frac{\sin 2q}{2q}\right) + (\sinh|p|)^2\left(1+\frac{\sin 2q}{2q}\right) + \frac{|p|r}{q}\cosh|p|\sinh|p|\left(1-\frac{\cos 2q}{2q}\right)\right]$$

in which $S$ is the cross section area of the guide ($S = a.b$) and $Z$ is the wave impedance:

$$Z = \sqrt{\frac{\mu_0}{\varepsilon_0}}\frac{\lambda_g}{\lambda_0}.$$

In the expression of $p_2$, some numerical applications show that the terms in $\sin 2q/q$ and in $\cos 2q/q$ can be neglected when the electric field is focused in region II, as described by curves 1 in Figs. 3 and 4.

The expressions of the power flow $P_2$ in region II containing the material to cure, and the power flow $P_1$ in the remaining

TABLE II
VARIATION OF THE RELATIVE POWER FLOW IN THE MATERIAL TO CURE, AS A FUNCTION OF THE PERMITTIVITY $\varepsilon'_1$ IN THE OUTER PART ($\varepsilon'_2 = 10$; $c/a = 0.27$)

| $\varepsilon'_1$ | 1 | 2 | 4 | 6 | 8 | 10 |
|---|---|---|---|---|---|---|
| $\frac{P_2}{P_1+P_2}$ | 0.84 | 0.82 | 0.77 | 0.70 | 0.59 | 0.44 |

part of the guide (regions I and III) are

$$P_1 = \frac{p_1}{p_1+p_2}P_0$$
$$P_2 = \frac{p_2}{p_1+p_2}P_0.$$

The relative power flow $P_2$ in region II, expressed as a ratio of the total power flow $P_0 = P_1 + P_2$ and as a function of $\varepsilon'_1$ is shown in Tables I and II for two values of $\varepsilon'_2$.

Since a good efficiency for the utilization of the incident power is obtained with the ratio $P_2/(P_1 + P_2)$ as high as possible, it is clear that the parameter $\varepsilon'_1$ should be as low as possible. The same conclusion as in the preceding paragraph is again found for the focusing of the electric field. It is important to emphasize that this information is necessary for the buildup of a homogeneous and optimal process.

### C. Higher Order Modes

Considering the question of higher order modes, the conditions of transmission of the $\mathrm{TE}_{02}$ and $\mathrm{TE}_{03}$ modes (first and second higher modes) are examined. The consideration of these conditions allows the realization of a dielectric mold, which eliminates the ability for a higher order mode to travel in the applicator, (i.e., which makes vanishing higher order modes eventually excited by the interfaces). Thus, the cutoff frequencies of $\mathrm{TE}_{02}$ and $\mathrm{TE}_{03}$ modes must be higher than the frequency of the incident wave $f_0$ (commonly 2.45 GHz). The cutoff frequency relations are easily found by setting $b = 0$ in (3) and (4); using (5) and (6), the transcendental equations which give the cutoff frequencies of the modes are

$\mathrm{TE}_{02}$ :

$$\frac{1}{\sqrt{\varepsilon'_1}}\tan\left(\pi\frac{a-c}{\lambda_c}\sqrt{\varepsilon'_1}\right) = -\frac{1}{\sqrt{\varepsilon'_2}}\tan\left(\pi\frac{c}{\lambda_c}\sqrt{\varepsilon'_2}\right) \quad (8)$$

$\mathrm{TE}_{01}$ and $\mathrm{TE}_{03}$ :

$$\frac{1}{\sqrt{\varepsilon'_1}}\tan\left(\pi\frac{a-c}{\lambda_c}\sqrt{\varepsilon'_1}\right) = \frac{1}{\sqrt{\varepsilon'_2}}\cot\left(\pi\frac{c}{\lambda_c}\sqrt{\varepsilon'_2}\right). \quad (9)$$

The cutoff frequencies calculated from (8) and (9) for the $\mathrm{TE}_{01}$, $\mathrm{TE}_{02}$, and $\mathrm{TE}_{03}$ modes are shown in Figs. 5 and 6 as functions of three variables $c/a$, $\varepsilon'_1$, and $\varepsilon'_2$. The curves show that a weak value for the ratio $c/a$ provides a very small variation of the $\mathrm{TE}_{02}$-mode cutoff frequency and a strong variation of the $\mathrm{TE}_{03}$ cutoff frequency. Secondly, one can discriminate the mode transmitted by the applicator when $f_c$ is lower than the wave frequency (2.45 GHz, in this example). Fig. 7 gives the results for several values of the permittivity in the peripheral dielectric material and, therefore, the conditions for the propagation of the $\mathrm{TE}_{02}$ mode related to the thickness of region II of high permittivity with $\varepsilon'_2 = 4$, which is a usual value in organic matrix composite materials. Taking into account these conditions, one can determine the limit load of the applicator $(c/a)_{\mathrm{crit}}$ according to the value of permittivity in regions I and III. Thus, Fig. 8 shows the nonlinear variations of this limit load. It follows that beyond the value of 1.8 for $\varepsilon'_1$, the variation of $c/a$ (and, therefore, of the thickness of curing material) leads to hazardous conditions; conversely, a permittivity of 1.4 is already a good solution because the ratio $(c/a)_{\mathrm{crit}}$ is almost constant down to the permittivity 1.0.

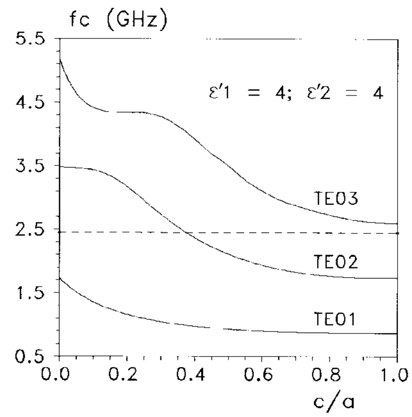


Fig. 5. Variation as a function of $c/a$ of the cutoff frequencies of the propagation modes $\mathrm{TE}_{01}$, $\mathrm{TE}_{02}$, and $\mathrm{TE}_{03}$. $\varepsilon'_1 = 1$, $\varepsilon'_2 = 4$.

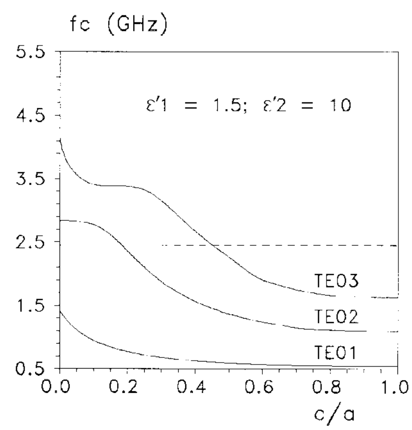


Fig. 6. Variation as a function of $c/a$ of the cutoff frequencies of the propagation modes $\mathrm{TE}_{01}$, $\mathrm{TE}_{02}$, and $\mathrm{TE}_{03}$. $\varepsilon'_1 = 1.5$, $\varepsilon'_2 = 10$.

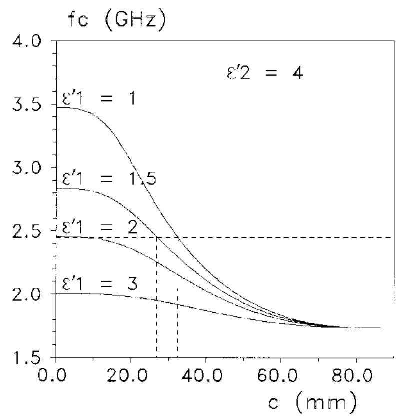


Fig. 7. Cutoff frequency versus $c$ and $\varepsilon_1'$ for the first higher order propagation mode, with $\varepsilon_2' = 4$.

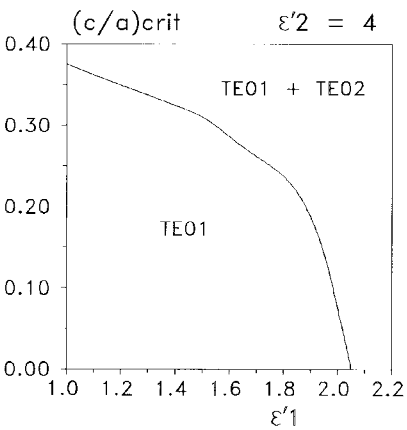


Fig. 8. Variation of $(c/a)_{\text{crit}}$ as a function of $\varepsilon_1'$, with $\varepsilon_2' = 4$.

### D. Wave Attenuation

It is assumed that the waveguide walls are of infinite conductivity. Thus, the wave attenuation is only caused by dielectric loss in load materials. The energy transfer in a multilayer system must be analyzed. Indeed, the wave attenuation along the applicator governs the dissipation of power in the material to cure, but the wave attenuation depends on the geometric and dielectric characteristics of the multilayer system.

Prior to determining the attenuation constant $\alpha$ of the whole system, one has to understand the physical significance of this quantity. The wave carries an available EM power. In an elementary volume, the length of which is $\partial z$, an elementary part $\partial P$ of this power is absorbed. Considering the electric-field constant along $\partial z$, the expression of $\partial P$ is

$$\partial P = \partial z \int_0^b \int_0^a \frac{\omega \varepsilon_0}{2} \varepsilon''(x,y) |\mathbf{E_x}(\mathbf{x},\mathbf{y})|^2 \, dx dy$$

for each value of the propagation coordinate $z$.

Assuming that only the fundamental mode $\mathrm{TE}_{01}$ is selected, with $\mathbf{E}$ parallel to $Ox$-axis and $\mathbf{E_x}$ constant along $Ox$, $\partial\ P$

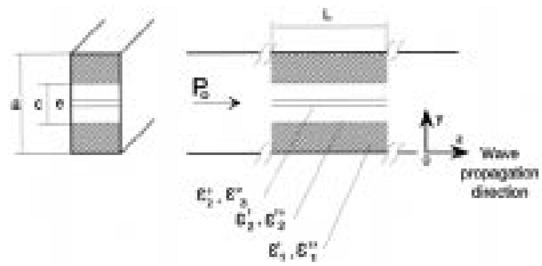


Fig. 9. Parameters used for the description of a five-layer applicator.

is given by

$$\partial P = \frac{b\omega\varepsilon_0}{2} \partial z \int_0^a \varepsilon''(y) |\mathbf{E_x}|^2 \, dy$$

$$or \frac{\partial P}{0} = \frac{b\omega\varepsilon_0}{2} \int_0^a \varepsilon''(y) |\mathbf{E_x}|^2 \, dy$$

with $\varepsilon''$ constant along $Ox$ too. Considering that electric and magnetic fields are exponentially decreasing functions of $z$ as $\exp(-\alpha z)$, the attenuation coefficient is such as

$$\frac{\partial P}{\partial z} = -2\alpha P.$$

To perform the optimization of the thermal process, the mold material must be less absorbent than the material to cure. Consequently, one has to separate the power dissipated inside the material and the power dissipated inside the dielectric mold material. Fig. 9 shows the dielectric characteristics of this central layer (permittivity $\varepsilon_2'$, loss factor $\varepsilon_3''$, thickness $e$), which represents the material to cure, alike on Fig. 1. The power flow through this layer is

$$P_3 = \frac{p_3}{p_1 + p_2} P_0$$

expression in which $p_3$ is

$$\begin{aligned} p_3 = \frac{r}{q}\Big( &(\sinh|p|)^2 \Big(\frac{e}{c} + \sin\Big(q\frac{e}{c}\Big)\cos q\Big(2 - \frac{e}{c}\Big)\Big) \\ &+ \Big(\frac{|p|r}{q}\Big)^2 (\cosh|p|)^2 (\frac{e}{c} - \sin\Big(q\frac{e}{c}\Big)\cos q\Big(2 - \frac{e}{c}\Big) \\ &+ 2\frac{|p|r}{q}\cosh|p|\sinh|p|\sin\Big(q\frac{e}{c}\Big)\sin q\Big(2 - \frac{e}{c}\Big)\Big). \end{aligned}$$

These expressions allow to determine the power $P_L$ lost in the structure

$$P_L = |\frac{\partial P}{\partial z}|.$$

$P_L$ is given by

$$P_L = b\omega\varepsilon_0 \int_0^{a/2} \varepsilon''(y) |\mathbf{E_x}(\mathbf{y})|^2 \, dy.$$

Using the electric-field expressions and after mathematical developments, it becomes

$$P_L = \frac{ab\omega\varepsilon_0 |\mathbf{E_0}|^2}{4(1+r)} (\varepsilon_1'' p_1 + \varepsilon_2''(p_2 - p_3) + \varepsilon_3'' p_3)$$

TABLE III
BALANCE SHEET OF ENERGY. INFLUENCE OF THE THICKNESS OF MATERIAL TO BE TRANSFORMED

| Thickness of the material to cure | $\alpha$ ($m^{-1}$) | $\frac{1}{2\alpha}$ (m) | $\frac{P_{d1}}{P_0}$ | $\frac{P_{d2}}{P_0}$ | $\frac{P_{d3}}{P_0}$ | $\frac{P_{transm}(*)}{P_0}$ |
|---|---|---|---|---|---|---|
| 1 mm | 0.865 | 0.58 | 0 | 17 % | 13 % | 71 % |
| 3 mm | 1.46 | 0,34 | 0 | 14 % | 30 % | 56 % |

(*) $P_{transm}$ is the power transmitted through a 200 mm long applicator.

and the final expression of the attenuation constant due to dielectric loss is

$$\alpha = \frac{1}{2}\frac{\lambda_g}{\lambda_0}\frac{2\pi}{\lambda_0}\frac{(\varepsilon_1'' p_1 + \varepsilon''(p_2 - p_3) + \varepsilon_3'' p_3)}{p_1 + p_2}.$$

The power dissipated in a length $L$ of loaded waveguide or applicator is

$$P_d = \omega\varepsilon_0 b \int_0^{a/2}\int_0^L \varepsilon'' |\mathbf{E}|^2(\mathbf{y},\mathbf{z})\mathbf{dydz}$$

or

$$P_d = \frac{ab\omega\varepsilon_0|\mathbf{E_0}|^2}{4(1+r)}\frac{1}{2a}(1 - e^{-2\alpha L})(\varepsilon_1'' p_1 + \varepsilon_2''(p_2 - p_3) + \varepsilon_3'' p_3).$$

Inside the three-layer system, the same definition of the dissipated power by means of detailed equations can be applied. Consequently, one obtains

$$P_{d1} = \frac{ab\omega\varepsilon_0|\mathbf{E_0}|^2}{4(1+r)}\frac{1}{2a}(1 - e^{-2\alpha L})(\varepsilon_1'' p_1)$$

$$P_{d2} = \frac{ab\omega\varepsilon_0|\mathbf{E_0}|^2}{4(1+r)}\frac{1}{2a}(1 - e^{-2\alpha L})(\varepsilon_2''(p_2 - p_3))$$

$$P_{d3} = \frac{ab\omega\varepsilon_0|\mathbf{E_0}|^2}{4(1+r)}\frac{1}{2a}(1 - e^{-2\alpha L})(\varepsilon_3'' p_3).$$

$P_{d1}$ corresponds to the power dissipated in I, $P_{d2}$ to the power dissipated in II, and $P_{d3}$ to the power dissipated in the curing material.

Table III reports the influence of the thickness of the material to cure on the power dissipated in each layer of the system, and on the power transmitted through a 200-mm-long applicator.

## IV. EXPERIMENTAL

This paper is devoted to a detailed electrical description of a microwave curing process of epoxy-based composite materials, completed with thermal considerations. Using another more simple description, an experimental verification was given in previous papers [7], [21].

The composite material to be cured was made of an epoxy resin reinforced with glass fibers. The epoxy resin was a stoichiometric mixture of diglycidyl ether of bisphenol-A (DGEBA) with dicyanodiamide (DDA) as a curing agent. The mold material was a silicone–glass composite Silirite Silicone. The external dielectric of low permittivity was a honeycomb polyimide material.

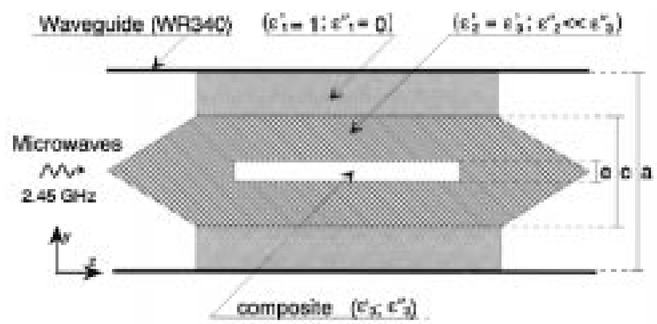


Fig. 10. Scheme of the final applicator (from [21]).

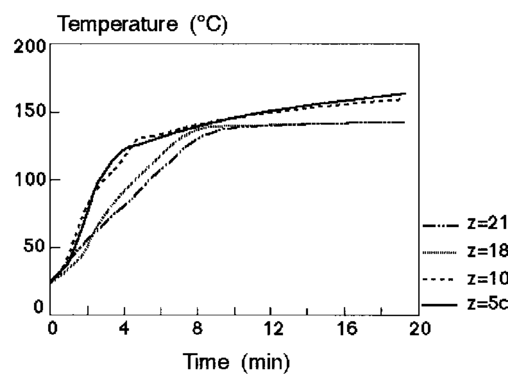


Fig. 11. Temperature–time variations in four points along the longitudinal axis of a DGEBA/DDA/glass fiber composite sample during microwave curing: all the points were cured with the same temperature–time profile, with only a time lag due to wave attenuation (from [21]).

A scheme of the microwave applicator is shown in Fig. 10. To maintain the traveling wave under fundamental mode $TE_{01}$ from the waveguide into the applicator, the operating part described in Fig. 9 was inserted between two tapered matched transition made of Silirite Silicone. The length of these transitions was 110 mm. A mechanical pressure of 10 bar was applied to the system.

The sample size was 250 $\times$ 33 $\times$ 3 mm. The microwave power was settled to 400 W for 20 min.

Temperature measurements were made by means of a four-way Luxtron Fluoroptic thermometer, in four points on the median line of samples. An example of the temperature–time profile is given in Fig. 11. A satisfactorily homogeneity of temperature was obtained: every point of the sample was

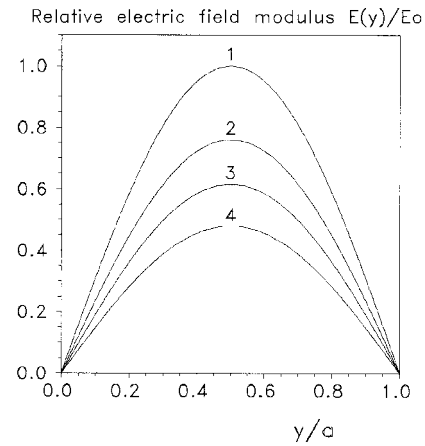


Fig. 12. Electric-field modulus profile along the larger side of an applicator filled up with a dielectric of permittivity $\varepsilon'$. 1: $\varepsilon' = 1$; 2: $\varepsilon' = 2$; 3: $\varepsilon' = 4$; 4: $\varepsilon' = 10$.

cured with the same temperature–time profile, with only a time lag due to wave attenuation. This assertion was confirmed by qualitative observations on thermosensitive paper replicas, showing the homogeneous temperature distribution, which suggested a homogeneous electric-field distribution, and by quantitative glass transition-temperature measurements in cured composites [21].

## V. Conclusion

The analysis presented in this paper shows the importance of an EM modeling for the buildup of a homogeneous optimized microwave curing process. It is shown that the efficiency of the microwave process depends on the achieved realization of the applicator loading. The conclusion of this theoretical work is that one can now manage the energy focusing and optimize the homogeneity of treatment by a suitable choice for the dielectric mold materials. This work shows that the dimensions and the dielectric characteristics of the material to be cured are the main elements determining the optimal thickness and dielectric characteristics of the mold materials. Moreover, since the power dissipation in a multilayer system can be determined, it is now possible to establish a balance sheet of energy in the applicator for the microwave processing of manufactured materials.

## Appendix

In a homogeneously filled rectangular waveguide, $\varepsilon'_1 = \varepsilon'_2 = \varepsilon'$ (relative permittivity); for the dominant mode $\mathrm{TE}_{01}$ the vector components of the EM field are

$$\mathbf{E_x} = \mathbf{E_0} \sin\left(\frac{\pi y}{a}\right)$$

$$\mathbf{H_y} = \mathbf{E_0} \frac{\lambda_0}{\lambda_g} \sqrt{\frac{\varepsilon_0 \varepsilon'}{\mu_0}} \sin\left(\frac{\pi y}{a}\right)$$

$$\mathbf{H_z} = \mathbf{E_0} \frac{\lambda_0}{\lambda_g} \sqrt{\frac{\varepsilon_0 \varepsilon'}{\mu_0}} \cos\left(\frac{\pi y}{a}\right).$$

The transverse electric profile is typically sinusoidal, as in Fig. 12, for different values of $\varepsilon'$. From the Poynting theorem, the power flow through the cross section is given by

$$P_0 = \frac{1}{2} \int\int (\mathbf{E_x} \Lambda \mathbf{H_y}\, dS).$$

Substituting the values of $|\mathbf{E_x}|$ and $|\mathbf{H_y}|$ and the propagation wavelength $\lambda_g$, and evaluating the integral, the final expression of the power is

$$P_0 = \frac{1}{4} \sqrt{\frac{\varepsilon_0 \varepsilon'}{\mu_0} \left(1 - (\frac{\lambda_0}{2a}^2\right)} |\mathbf{E_0}|^2 a.b.$$

## References


[1] A. Vaguine, “Microwave applicator with discoupled input coupling and frequency tuning functions,” U.S. Patent 4 446 874, May 8, 1984.

[2] W. Kim, “Electromagnetic field heating apparatus for curing resin/fiber composites in continuous pultrusion process,” U.S. Patent 4 777 707, Oct. 10, 1984.

[3] K. Yamamoto, [title unknown], Japanese Patent 60-135 230, July 18, 1985.

[4] C. Becheret, “Process and device for forming and polymerizing thermosetting plastic articles,” European Patent 0 347 299, June 12, 1989.

[5] M. Delmotte, L. Outifa, C. Moré, and H. Jullien, “Dispositif de traitement homogòne par micro-ondes de matériaux sous contrainte de pression mécanique,” French Patent 2 669 557, May 29, 1992.

[6] E. B. Manring and J. Asmussen, “Numerical calculations for single mode, continuous processing of rods and filaments,” *Polym. Mater. Sci. Eng.*, vol. 66, pp. 476–477, 1992.

[7] L. Outifa, H. Jullien, and M. Delmotte, “The microwave curing of large size epoxy-glass composite samples: How to make it homogeneous,” *Polym. Mater. Sci.* (Eng.), vol. 66, pp. 424–425, 1992.

[8] W. I. Lee and G. S. Springer, “Microwave curing of composites,” *J. Compos. Mater.*, vol. 18, pp. 387–409, 1984.

[9] B. Krieger, “Vulcanization of rubber, a resounding success for microwave processing,” *Polym. Mater. Sci. Eng.*, vol. 66, pp. 339–340, 1992.

[10] C. Yu and T. Chu, “Analysis of dielectric-loaded waveguide,” *IEEE Trans. Microwave Theory Tech.*, vol. 38, pp. 1333–1338, Sept. 1990.

[11] M. E. El-Shandwily and S. M. El-Dinary, “Traveling wave coherent light phase modulator,” *IEEE Trans. Microwave Theory Tech.*, vol. MTT-20, pp. 132–137, Feb. 1972.

[12] F. E. Gardiol, “Higher order modes in dielectrically loaded rectangular waveguides,” *IEEE Trans. Microwave Theory Tech.*, vol. MTT-16, pp. 919–924, Nov. 1968.

[13] N. Eberhardt, “Propagation in the off center $E$-plane dielectrically loaded waveguide,” *IEEE Trans. Microwave Theory Tech.*, vol. MTT-15, pp. 282–289, May 1967.

[14] P. H. Vartanian, W. P. Ayres and A. L. Helgesson, “Propagation in dielectric slab loaded rectangular waveguide,” *IEEE Trans. Microwave Theory Tech.*, vol. MTT-6, pp. 215–222, Apr. 1958.

[15] R. E. Collin, *Field Theory of Guided Waves*. New York: McGraw-Hill, 1960, ch. 6.

[16] L. G. Chambers, “Propagation in waveguides filled longitudinally with two or more dielectrics,” *Br. J. Appl. Phys.*, vol. 4, pp. 39–45, Feb. 1953.

[17] N. Marcuvitz, *Waveguide Handbook*. New York: McGraw-Hill, 1951.

[18] T. Moreno, *Microwave Transmission Design Data*. Norwood, MA: Artech House, 1989, ch. 11.

[19] W. E. Hord, “Continuously tapered dielectric matching transitions for waveguides,” Ph.D. dissertation, Dept. Elect. Eng., Univ. Missouri, Rolla, MO, 1966.

[20] L. Outifa, “Contribution au génie de l’élaboration par micro-ondes de matériaux composites à matrice polymère de dimensions supérieures à la longueur d’onde. Aspects électromagnétique et thermique,” Ph.D. dissertation, Dept. Chimie Appliquée et Génie des Procédés Industriels, Univ. P. et M. Curie, Paris, France, 1992.

[21] L. Outifa, H. Jullien, C. Moré, and M. Delmotte, “Buildup and optimization of a homogeneous microwave curing process for epoxy-glass composites,” *Ind. Eng. Chem. Res.*, vol. 34, pp. 688–698, 1995.

**Lhoussain Outifa** was born in Ghazoine, Talsint, Morocco, in 1964. He received the engineering degree from the Ecole Nationale Supérieure de Chimie de Paris, Paris, France in 1989, and the Ph.D. degree from the Pierre et Marie Curie University, Paris, France, in 1992.

From 1989 to 1992, he was involved in a research program at the Centre National de la Recherche Scientifique (CNRS, Thiais, near Paris), where he investigated the use of microwaves to cure large-sized composite materials. From 1992 to 1994, he developed a pilot workshop for the microwave processing of a composite piece for motorcar industries. He is presently involved with a hydrometallurgical process of cobalt ores in Morocco. He is a co-author for several papers and holds three patents dealing with the buildup of the microwave curing process.

Dr. Outifa was awarded the Prize of the Best Thesis in Electrothermy from the Club Electrothermie Enseignement in 1993.

**Michel Delmotte** was born in Roncq, Nord, France, in May 1946. He received the D.Sc. degree in biophysics in 1975, studying the applications of nonequilibrium thermodynamics to the biological membrane behavior.

Since 1981, he has been concerned with microwave dielectric measurements in organic materials. From 1988 to 1994, he was managing a research program investigating the use of microwave power for the processing of polymeric composite materials. Since 1994, he has been working at the Ecole Nationale Supérieure d'Arts et Métiers, Paris, France.

**Henri Jullien** was born in Mâcon, Saône-et-Loire, France, in 1940. He studied chemistry at the Ecole Nationale Supérieure de Chimie de Paris, graduated as a chemical engineer in 1963, and received the D.Sc. degree from the Centre National de la Recherche Scientifique (CNRS), Paris, France, in 1970

He then investigated electrochemical properties in polyurethane films, in relation with the use of polyurethane resins in anticorrosion paints. Since 1978, he has been investigating the energy transfer to polymeric materials by means of microwaves, both from a molecular and from a macroscopic point of view, and especially the action of microwaves onto the crosslinking chemical reactions in thermosetting polymers. He has been developing the microwave processing of polymer composites (along with his co-author, M. Delmotte), and since 1994, has been working at the Ecole Nationale Supérieure d'Arts et Métiers, Paris, France.